Mon. Not. R. Astron. Soc. **373,** 715–728 (2006) doi:10.1111/j.1365-2966.2006.11053.x

The stellar content of the isolated transition dwarf galaxy DDO210⋆

Alan W. McConnachie,[1]† Nobuo Arimoto,[2] Mike Irwin[3] and Eline Tolstoy[4]

[1]*Department of Physics and Astronomy, University of Victoria, Victoria, BC V8P 1A1, Canada*
[2]*National Astronomical Observatory of Japan, 2-21-1 Osawa, Mitaka, Tokyo 181-8588, Japan*
[3]*Institute of Astronomy, University of Cambridge, Madingley Road, Cambridge CB3 0HA*
[4]*Kapteyn Institute, University of Groningen, Postbus 800, 9700AV Groningen, the Netherlands*

Accepted 2006 September 8. Received 2006 August 31; in original form 2006 July 7

ABSTRACT

We use Subaru Suprime-Cam and VLT FORS1 photometry of the dwarf galaxy DDO210 to study the global stellar content and structural properties of a transition-type galaxy (with properties intermediate between dwarf irregular and dwarf spheroidal systems). This galaxy is sufficiently isolated that tidal interactions are not likely to have affected its evolution in any way. The colour–magnitude diagrams of DDO210 show a red giant branch (RGB) population (with an RGB bump), a bright asymptotic giant branch population, a red clump, young main-sequence stars and blue-loop stars. The youngest stars formed within the last 60 Myr and have a distinct radial distribution compared to the main population. Whereas the overall stellar spatial distribution and H I spatial distribution are concentric, the young stars are offset from the centre of DDO210 and are coincident with a 'dent' in the H I distribution. The implied recent star formation rate required to form the young population is significantly higher than the derived current star formation rate, by a factor of >10.

Most of the stars in DDO210 are found in a red clump, and its mean *I*-band magnitude suggests that the majority of stars in DDO210 have an average age of 4^{+2}_{-1} Gyr. Given this age, the colour of the RGB implies a mean metallicity of [Fe/H] $\simeq -1.3$. By comparing the shape of the red clump with models for a variety of star formation histories, we estimate that an old (>10 Gyr) stellar population can contribute $\sim$20–30 per cent of the stars in DDO210 at most. The unusual star formation history of DDO210, its low-mass estimate and its isolated nature, provide insight into how star formation proceeds in the lowest mass, unperturbed, dwarf galaxy haloes.

Key words: galaxies: dwarf – galaxies: individual: DDO210/Aquarius – Local Group – galaxies: stellar content – galaxies: structure.

1 INTRODUCTION

The stellar, chemical and structural evolution of dwarf galaxies is believed to depend strongly on environment. In the Local Group, dwarf spheroidal (dSph) galaxies are preferentially found as satellites to M31 and the Milky Way (MW), whereas dwarf irregular (dIrr) galaxies are preferentially found in isolated locations. This was first highlighted by Einasto et al. (1974) (see also van den Bergh 1999), and implies that the presence of a nearby large galaxy causes morphological changes in its satellites, primarily via the loss of gas by a combination of tidal stirring and ram-pressure stripping (Mayer et al. 2001a,b; Grebel, Gallagher & Harbeck 2003). Tidal effects from the large galaxies may also be responsible for star formation episodes in their satellites, by triggering compression of their gas. However, the orbital properties of the MW satellites are difficult to determine, and so correlations between star formation histories (SFHs) and orbital phase have yet to be robustly demonstrated.

The stellar evolution of dwarf galaxies is also interesting from a cosmological viewpoint, in particular regarding the missing satellites problem. A long standing problem faced by theories of galaxy formation in the cold dark matter paradigm is that purely gravitational simulations predict that there should be around an order of magnitude more dwarf galaxies in the Local Group, particularly around the MW and M31 (Kauffmann, White & Guiderdoni 1993; Klypin et al. 1999; Moore et al. 1999). As recent results are demonstrating, it appears as if there are numerous low surface brightness dwarf galaxies which have yet to be discovered (Zucker et al. 2004, 2006a,b; Willman et al. 2005; see also Belokurov et al. 2006; Willman et al. 2006) although it is unclear if these discoveries will increase the observed number by the required order of magnitude. One potential solution to this difficulty is that not all dwarf

⋆Based in part on data collected at Subaru Telescope, which is operated by the National Astronomical Observatory of Japan

†E-mail: alan@uvic.ca

galaxy-scale dark matter haloes can accrete and retain gas to form stars, and instead reionization can prevent certain haloes from forming a luminous component (Bullock, Kravtsov & Weinberg 2000; Kravtsov, Gnedin & Klypin 2004; Ricotti & Gnedin 2005; Gnedin & Kravtsov 2006). Susa & Umemura (2004) showed that star formation is suppressed significantly by the effects of reionization, but that sufficiently massive dwarf galaxies are able to form stars eventually because the baryons are self-shielded.

Even in these cosmological scenarios, the influence of tidal effects from the MW and M31 can play important roles in determining the evolution of a dwarf galaxy. Indeed, tidal effects present one of the greatest uncertainties in our interpretation of dwarf galaxy evolution, and it is therefore of considerable interest to study dwarf galaxies unaffected by the presence of an external tidal field. DDO210 ($20^{\rm h}46^{\rm m}51\overset{\rm s}{.}8$, $-12^\circ50'53''$) is one of the most isolated galaxies in the Local Group. It was discovered at the limits of detectability on the Palomar Sky Survey by van den Bergh (1959), in the constellation of Aquarius. Fisher & Tully (1975) detected it in H I 21-cm emission, and later assigned it an arbitrary distance modulus of $(m - M) = 25$ mag, based upon some general similarities to the Local Group galaxy WLM. For a long time DDO210 remained very poorly studied, and Marconi et al. (1990) were the first to resolve its individual stars, to a limiting magnitude of $V = 23.5$ mag.

Despite the lack of any distance measurement, DDO210 was considered to be a member of the Local Group from soon after its discovery (e.g. Yahil, Tammann & Sandage 1977; van den Bergh 1979; de Vaucouleurs, de Vaucouleurs & Buta 1983). Greggio et al. (1993) were the first to estimate an independent distance to this galaxy, $(m - M) \simeq 28$ mag ($d \simeq 4.3$ Mpc), placing it well beyond the zero velocity surface of the Local Group. However, more recent distance measurements by Lee et al. (1999) (L99), Karachentsev et al. (2002) (K02) and McConnachie et al. (2005) (M05), all of which are based upon the tip of the red giant branch (TRGB; Lee, Freedman & Madore 1993), show that DDO210 is, in fact, located at $\sim$1 Mpc from the Milky Way (MW), on the periphery of the Local Group. This places DDO210 at slightly over 1 Mpc from M31. The free-fall time-scale of DDO210 into M31 or the MW is

$$t_{ff} \simeq 14.4\ {\rm Gyr} \left(\frac{r}{1\ {\rm Mpc}}\right)^{3/2} \left(\frac{M}{10^{12}\ {\rm M}_\odot}\right)^{-(1/2)}, \quad (1)$$

i.e. of the order of a Hubble time. It is clearly not, and never has been, a satellite of either of the dominant members of the Local Group.

Mateo (1998) classified DDO210 as a transition-type galaxy, with properties intermediate to those which are usually ascribed to dSph and dIrr galaxies. Its magnitude is $M_V \simeq -10.6$ mag (L99), making it the faintest dwarf galaxy in the Local Group with a significant gaseous component. Despite the presence of this gas, an Hα study of this galaxy (van Zee, Haynes & Salzer 1997) shows that there is no current star formation. This is rather unusual, given that L99 showed that this galaxy contains a significant number of young stars, and that the central portion of this galaxy has undergone a recent enhancement in its star formation rate (SFR) in the last few hundred Myr.

Begum & Chengalur (2004) conducted deep, high-velocity resolution H I 21-cm observations of DDO210 with the Giant Meterwave Radio Telescope. They found that the velocity field of this galaxy is quite regular, and has a corrected peak rotation velocity of $\sim$16 km s^{-1}. When incorporated into mass models of DDO210, this implies a total dynamical mass of the order of 10^{7-8} M$_\odot$, comparable to many of the dwarf satellites of M31 and the MW. Since DDO210 is so isolated, it offers an excellent opportunity to study the stellar evolution of a dwarf galaxy in the absence of any significant external tidal fields.

In this paper, we analyse deep, global, multicolour photometry of DDO210, obtained with Subaru Suprime-Cam and VLT FORS1. We analyse the stellar content, structural properties and SFH of this galaxy, and show that it is dominated by an intermediate-age stellar population with an average age of $\sim$4 Gyr. In Section 2, we discuss our Subaru Suprime-Cam and VLT FORS1 photometric data sets and the data-reduction procedure. In Section 3, we present deep, global, CMDs of the stellar populations of DDO210, and use these to derive the properties of its multiple stellar populations. We compare the CMDs with synthetic models of various SFHs and use this to estimate the possible contribution from an ancient ($\gtrsim$10 Gyr) stellar component. In Section 4, we analyse the global structure of DDO210, in terms of its integrated properties and the radial profiles of the various stellar populations, and we compare these to the global distribution of H I from previous Very Large Array (VLA) observations by Young et al. (2003). We discuss the nature of DDO210 in light of these new results in Section 5, and we summarize our findings in Section 6. We assume an extinction value towards DDO210 of $E(B - V) = 0.052$ (Schlegel, Finkbeiner & Davis 1998).

2 THE PHOTOMETRIC DATA SETS

2.1 Subaru Suprime-Cam

During the nights of 2005 August 3rd–5th, we observed with the 34×27 arcmin^2 Suprime-Cam wide-field camera on the Subaru Telescope obtaining Johnson–Cousins V and $I_{\rm c}$-band imaging of several Local Group dwarf galaxies which are not satellites of the Milky Way (see McConnachie, Arimoto & Irwin, 2006). Conditions were uniformly excellent, being photometric throughout and with typical seeing of 0.5 arcsec. For DDO210, we exposed for a total of 4320 s in V and 7200 s in $I_{\rm c}$, split as 12×360 s and 30×240 s dithered subexposures, respectively. The telescope was typically offset $\sim$20 arcsec between subexposures. Although the V-band DDO210 observations were taken at relatively high airmass (1.5–2.2), the final stacked images still have subarcsec seeing, averaging 0.82 arcsec over the whole array. For the $I_{\rm c}$-band images, mostly taken at lower airmass, the seeing in the stacked image averages 0.51 arcsec. The reader is referred to McConnachie, Arimoto & Irwin (in preparation) for details of the data-reduction process. Fig. 1 shows the reduced Suprime-Cam images of DDO210.

We cross-correlate the Suprime-Cam photometry with our earlier multicolour Isaac Newton Telescope Wide Field Camera photometry of DDO210 (M05), for which we know the colour transformations into the Landolt system.[1] This ensures our new photometry is on the same systems as our previous photometry. By only considering those objects reliably identified as stellar in all four sets of observations, we find

$$\begin{aligned} V &= V' + 0.030\,(V - I) \\ I &= I_{\rm c} - 0.088\,(V - I)\,, \end{aligned} \quad (2)$$

where we now use V' to denote the original Subaru V filter. The transformations are small, and we apply these colour equations to our Suprime-Cam data.

We have compared our VI photometry to the photometry of L99, for bright stars with $V < 22$ over their entire field. Based upon tight

[1] http://www.ast.cam.ac.uk/wfcsur/technical/photom/colours

spatial coincidence, we confidently identify 26 common stars, which have a mean $\Delta V = 0.038$ (our photometry minus L99 photometry). This is small in comparison to the various sources of error; for example, the calibration error in the photometry of L99 is given as 0.04–0.05 mags, and the uncertainty in the zero-point of our photometry is typically $\sim$0.02 mag. Thus, we conclude that our photometry is in good agreement with L99, which has itself been shown to agree well with the earlier studies of Greggio et al. (1993) and Hopp & Schulte-Ladbeck (1995).

2.2 VLT FORS1

We have also included in our analysis deep B- and R-band imaging of the centre of DDO210 taken during excellent stable photometric conditions in 1999 August with the newly commissioned FORS1 instrument on UT1 at the VLT (P. I. E. Tolstoy). These filters were chosen to match the wavelength range in which the instrument is most sensitive and preliminary results from these observations have been presented in Tolstoy et al. (2000). The data were originally reduced using standard procedures, and the stacked B and R-band images were subsequently processed in the same way as the Subaru data. This produced B- and R-band detected objects and a combined B, R catalogue.

3 THE STELLAR POPULATIONS OF DDO210

Figs 2 and 3 show the V versus $(V - I)$ and I versus $(V - I)$ CMDs for DDO210, respectively, constructed from the innermost 4×4 arcmin^2 of our Suprime-Cam field. Also shown are the corresponding CMDs for a reference area, which lies outside the innermost 7.5×7.5 arcmin^2 of the Suprime-Cam field, beyond the limits of DDO210. Fig. 4 shows the B versus $(B - R)$ CMD from the FORS1 field. DDO210 is an intrinsically very faint system, and the CMDs are correspondingly rather sparse. However, several different stellar populations can be identified in these diagrams, namely the following.

(i) A Galactic foreground sequence. At the brightest magnitudes this has a colour of $(V - I) \simeq 0.7$, becoming redder at fainter magnitudes. This feature is unassociated with DDO210.

(ii) A relatively thin RGB, starting at $I \sim 21$ mag, with a colour of $(V - I) \sim 1.1$ mag at $V \sim 25$ and $(V - I) \sim 1.4$ mag at $V \sim 23$.

(iii) A red clump of stars, most clearly visible at $B \simeq 25.8$ mag and $(B - R) \simeq 1.2$ mag;

(iv) Bright main-sequence stars, at $V \gtrsim 23$ mag and $(V - I) \sim -0.2$ mag.

(v) Bright blue-loop stars, at $V \gtrsim 21$ mag and $(V - I) \sim 0.2$ mag.

In this section, we analyse each of these stellar evolutionary phases in turn, to determine what they are able to reveal about the SFH of DDO210, in particular regarding the ages and metallicities of the populations present. In order to do this successfully, we first revisit the distance estimate to this galaxy.

3.1 The distance to DDO210 revisited

Recent distance estimates to DDO210 have all made use of the TRGB. Physically, this is the point at which low-mass RGB stars undergo the core helium flash, which begins their core helium-burning phase and takes them off the RGB. For metal-poor ([Fe/H] < -0.5), old (>2Gyr) stellar populations, the I-band magnitude of this point has been shown to be a good standard candle (e.g. Da Costa & Armandroff 1990; Lee et al. 1993; Barker, Sarajedini & Harris 2004), and is marked by a discontinuity in the I-band luminosity function. This discontinuity can be found using a variety of methods, such as edge detection algorithms (Lee et al. 1993; Sakai, Madore & Freedman 1996), or maximum-likelihood techniques (Méndez et al. 2002; McConnachie et al. 2004). The reliability of these methods is greatly increased when used on a well-populated RGB. As noted by M05, this is not the case for DDO210. These authors identify two possible locations for the TRGB, favouring their fainter measurement at $I = 21.21 \pm 0.04$ mag. L99 and K02 derived a different value for the TRGB, at $I = 20.95 \pm 0.10$ mag and 20.91 ± 0.05 mag, respectively. This is closer to the second location identified by M05 as the possible TRGB of DDO210, at $I \sim 20.8$ mag.

Although all of the above measurements place DDO210 at $\sim$1 Mpc, the significant disagreement between M05 and L09 + K02 warrants further investigation. To this end, we examine how the TRGB region of the I-band CMD of DDO210, from our Suprime-Cam data, varies as we apply different spatial cuts. We expect that the derived value of the TRGB should remain relatively constant regardless of the spatial cuts applied so long as the dominant population belongs to DDO210, with the caveat that cuts which contain fewer stars will be more strongly affected by small number statistics. The left-hand panel of Fig. 5 shows an enlargement of the I-band CMD from Fig. 3 around the location of the TRGB. The dashed lines approximately bracket the RGB locus. The arrows indicate the values of the TRGB as derived by K02 (top panel), L99 (middle panel) and M05 (bottom panel). The middle panel shows the same region of the CMD using only stars within the innermost 4×4 arcmin^2 of the Suprime-Cam field, and the right-hand panel is the same but using stars within the innermost 2×2 arcmin^2. This figure illustrates well the difficulty in determining the location of the TRGB for an intrinsically faint system with few bright RGB stars.

Fig. 5 shows that the grouping of stars which defines the L99 and K02 TRGB location has completely disappeared in the smallest field, and is very weak in the middle field. In contrast, the location identified by M05 is clear for all of the spatial cuts used, and the RGB is relatively evenly populated below this point in each field. Even for a small number of stars, we expect that the RGB luminosity function will be representatively sampled over its full magnitude range. It seems most likely, therefore, that the measurement by M05 provides the most robust estimate of the TRGB of this galaxy, and implies a distance modulus of $(m - M)_o = 25.15 \pm 0.08$ mag ($d = 1071 \pm 39$ kpc). If this is the case, however, then the grouping of stars identified by K02 and L99 as the brightest RGB stars cannot belong to this population.

We investigate whether the stars immediately brighter than the TRGB are foreground stars by examining their number density. Using a colour cut of $1.3 < (V - I) < 1.7$ and $20.80 < I < 21.21$ to isolate these stars, we find that there are 25 ± 5, 17 ± 4 and 5 ± 2 in the 8×8, 4×4 and 2×2 arcmin^2 fields, respectively. The uncertainties are Poisson errors. In comparison, a representative foreground field offset 10 arcmin from the centre of DDO210 has $5 \pm 2, 2 \pm 1$ and 0 stars, respectively, which satisfy these colour cuts. Thus, the number density of these stars in our DDO210 fields is too large to be explained by a foreground population alone.

We believe it likely that these stars represent bright, intermediate-age, upper asymptotic giant branch (AGB) stars. The stars occupy the correct locus in the I-band CMD to belong to this population, and the corresponding positions of these stars (satisfying the same colour cuts as before) in the FORS1 data are highlighted in Fig. 4. The majority of these stars are tightly grouped slightly to the red and brighter than the RGB, again suggesting that they belong to an

evolved AGB population. We show in the next section that this is consistent with the average age of the stellar population. We also note that, although the overall number of these stars is smallest in the smallest field in Fig. 8, this is probably due only to the reduced area. The spatial distribution of these stars is shown in Fig. 12, as open star symbols overlaid on the grey-scale stellar density map. They are loosely concentrated in the main body of DDO210, and broadly follow a similar distribution to the overall stellar population.

3.2 The candidate asymptotic giant branch population

In the metal-poor Galactic globular clusters, which consist nearly exclusively of old stellar populations, no stars are observed brighter than the TRGB with colours similar to the RGB. This is because the AGB population terminates at a magnitude comparable to, or less than, the TRGB. In younger stellar populations, the envelope mass of AGB stars is larger and so they have the ability to evolve to brighter luminosities, and can exceed the luminosity of the TRGB. Thus, the presence of stars at luminosities brighter than the TRGB, with colours similar to the RGB, is usually interpreted as evidence for the existence of an intermediate-age population.

The brightest of the candidate AGB stars in DDO210 identified in Section 3.1 has a magnitude of $I = 20.93$ mag and a colour of $(V - I) = 1.49$ mag. Correcting for extinction and the distance to DDO210, this corresponds to an absolute magnitude of $M_I = -4.32$ mag and a colour of $(V - I)_{\rm o} = 1.42$ mag. Using the *VI* bolometric correction derived by Da Costa & Armandroff (1990), we find that $M_{\rm bol} = -4.86$ mag for the brightest candidate AGB star. This number should be considered an upper limit, due to the difficulties in distinguishing between an evolved AGB star and a foreground star with a similar colour and magnitude. A lower limit on the luminosity can be obtained by using the magnitude of the TRGB; adopting the same colour as before, we find $M_{\rm bol} = -4.58$ mag. We therefore adopt $M_{\rm bol} \simeq -4.6 - -4.9$ mag for the brightest candidate AGB stars in DDO210.

A recent paper by Rejkuba et al. (2005) has a very useful comparison between the $M_{\rm bol}$ of the brightest AGB star in a selection of dwarf galaxies with the time since the period of star formation which produced the star. Mould & Aaronson (1979, 1980) were the first to make use of such a relation, made possible by the monotonically decreasing luminosity of AGB stars with age, and this has more recently been theoretically quantified by Stephens & Frogel (2002). By comparing DDO210 with those galaxies listed in Rejkuba et al.'s table 7, we find that the magnitude of the brightest AGB stars is very similar to those in Carina and Andromeda II. For Carina, the last period of star formation was some 3 Gyr ago (Hurley-Keller, Mateo & Nemec 1998). Fig. 19 of Rejkuba et al. makes explicit their empirical relation between the bolometric luminosity of the brightest AGB star and the age of the star. The comparison of our data to this figure reveals that the bolometric magnitude of the brightest candidate AGB stars in DDO210 implies ages between 3 and 6 Gyr. These numbers should be interpreted with care, as our analysis is based on a very few stars and we are unable to distinguish between actual AGB stars and foreground. Nevertheless, these numbers suggest that star formation was ongoing in DDO210 in the last 3–6 Gyr.

3.3 The main sequence and blue loop: evidence of recent star formation

The presence of a main-sequence population and blue-loop stars at $(V - I) < 0$ in the CMD of DDO210 reveals the presence of stars which are significantly younger than those represented by the evolved AGB stars. Fig. 6 is the V versus $(V - I)$ shown in Fig. 2, with isochrones from Girardi et al. (2002) overlaid. We have shifted these isochrones to the distance and reddening of DDO210. These isochrones correspond to a metallicity of [Fe/H] $= -1.3$ (Section 3.5) and ages of 60, 100, 180, 250, 350 and 550 Myr. The magnitude of the brightest main-sequence and blue-loop stars depends primarily on age, and is relatively independent of metallicity. They can, therefore, be used as a crude age indicator.

The dashed line in Fig. 6 marks the approximate locus of blue-loop stars as defined by the isochrones, and it is clear that they trace the blue-loop stars in DDO210 very well. The corresponding expected locus of red supergiants is, unfortunately, obscured by the presence of foreground stars with the same colours. The main sequences of the isochrones match the main-sequence population of DDO210 with notable success. There are a few main-sequence stars which are too blue to match the positions of the isochrones, and it is very possible that a younger isochrone ($\sim$30 Myr) is required to match this population. This is what L99 assumed which led them to conclude that there were stars as young as 30 Myr in DDO210. Given the various uncertainties which go into modelling stellar populations which inevitably produce variations between different isochrone sets, and photometric errors, we prefer to conclude that this comparison shows that DDO210 has stars which formed within the last 60 Myr. As noted in Section 1, this is rather unusual given that star formation in DDO210 is now observed to be completely dormant (van Zee et al. 1997).

3.4 The red clump, and limits on an old population

3.4.1 The magnitude and colour of the red clump

The most populated region of the CMDs shown in Figs 2–4 is the red clump, which stands out most clearly in Fig. 4. Defining the locus of the red clump as $25.45 < B < 26.15$ mag, $1 < (B - R) < 1.5$ mag, we find that $\sim(1/4)$ of all stars detected in the FORS1 field belong to this feature. The red clump is a composite feature in a CMD, of which the large majority of stars are metal-rich, massive, core helium-burning stars. These are indicative of an intermediate-age population (2–10 Gyr). RGB stars and red HB stars can also contribute to this feature.

A large amount of theoretical modelling of the red clump has been conducted in recent years (e.g. Cole 1998; Girardi et al. 1998; Girardi & Salaris 2001), motivated by claims that the mean magnitude of the red clump can be used as a standard candle (Paczynski & Stanek 1998; Udalski et al. 1998). This has resulted in a relatively good understanding of the behaviour of the luminosity and colour of the red clump on the age and metallicity of the population. In particular, Girardi & Salaris (2001) calculated the mean *I*-band magnitude of the red clump, $M_I^{\rm RC}$, as a function of age and metallicity. The form of this dependency is given in their equation (3), and is an integral over a function of the initial mass function. It transpires that $M_I^{\rm RC}$ is mostly dependent upon age, whereas the colour of the red clump, $(V - I)_{\rm o}^{\rm RC}$, is mostly dependent on metallicity. We can therefore use the properties of the red clump to put limits on the SFH of DDO210.

The models of Girardi & Salaris (2001) are formulated in the V and I filters. As it stands, the Suprime-Cam $I_{\rm c}$ data easily reaches to below the red clump, while the V'-band exposure is barely deep enough to fully sample this feature. This therefore leads to some difficulty in accurately determining $M_I^{\rm RC}$ and $(V - I)_{\rm o}^{\rm RC}$ using this single data set. The FORS1 data, on the other hand, are deep enough to fully sample the red clump. In order to push the V'-band data deep enough

Figure 1. The V- and I_c-band Suprime-Cam fields, centred on DDO210. Each field measures 34×27 arcmin^2. North is to the top, and east is to the left.

to compare the red clump properties to these models, we incorporate our deep FORS1 *BR* photometry into our Suprime-Cam data. To do this, we cross-correlate the two data sets and identify those stars which are reliably detected in all four filters, and which have small errors in their photometry ($\leqslant$0.05 mag). We then calculate the linear transformation between $(V-I)_o$ and $(B-R)_o$, shown in Fig. 7, and find

$$(V-I)_o = 0.652(B-R)_o. \quad (3)$$

When combined with equation (2), this gives

$$M_V = M_{I_c} + 0.593(B-R)_o$$
$$M_I = 1.096M_{I_c} - 0.097M_V. \quad (4)$$

We use these new transformations to calculate V and I magnitudes for those stars which are detected in the B, R and I_c filters, but not V'. The new V versus $(V-I)$ CMD derived in this way is shown in the left-hand panel of Fig. 9, and the red clump is now clearly visible and much better defined than in Fig. 3.

Fig. 8 shows the M_V and M_I luminosity functions for DDO210. The luminosity functions have not had a foreground correction applied, as for the purposes intended here this makes no practical difference since the red clump massively outnumbers any foreground component with the same colours. We measure the mean magnitude of the red clump by fitting a Gaussian to the luminosity functions in the region of the red clump, and taking the peak of the Gaussian as the mean magnitude of the clump. The resulting fits are shown as dot–dashed lines in Fig. 8. We find that $M_I^{RC} = -0.51 \pm 0.10$ mag, $M_V^{RC} = 0.27 \pm 0.14$ mag and $(V-I)_o^{RC} = 0.78 \pm 0.05$. The uncertainties in M_I^{RC} and M_V^{RC} include the uncertainty in the distance modulus of DDO210.

Fig. 1 of Girardi & Salaris (2001) shows the dependency of M_I^{RC} on age for a range of metallicities. By comparing the value of $M_I^{RC} = -0.51 \pm 0.10$ mag for DDO210 with this graph, we find that *the red clump in DDO210 belongs to a population with an average age equal to or younger than ∼6 Gyr old* (4^{+2}_{-1} Gyr). For a given metallicity, there are as many as three solutions for M_I^{RC}. One of these solutions corresponds to a stellar population older than ∼2 Gyr, while the remaining solutions correspond to populations younger than ∼2 Gyr. The average metallicity of the dominant population, as implied by $(V-I)_o^{RC} = 0.78 \pm 0.05$, is $-2.0 \lesssim$ [Fe/H] $\lesssim -1.3$, where the lower limit is least well constrained.

3.4.2 *The shape of the red clump*

The *magnitude* of the red clump implies that the majority of stars in DDO210 belong to an intermediate-age population, and so far we have found no evidence of an old population in this galaxy. To try to better constrain the range of ages of stars present in DDO210, we now compare the *shape* of the red clump to model CMDs with a range of SFHs. We use the web-based synthetic CMD tool IAC-STAR,[2] developed by Aparicio & Gallart (2004). The user supplies the SFH, chemical enrichment law, initial mass function (IMF) and binary fraction (and mass ratio) for the stellar population they want to model, and has a choice of stellar evolution libraries and bolometric correction libraries which can be used. The program then does a Monte-Carlo simulation of the evolution of N stars, with a distribution of properties chosen to be consistent with the user-supplied input, and outputs the luminosities of these stars at the present day in several filter systems.

The modelling of CMDs is prone to many uncertainties and degeneracies, such as the evolutionary tracks used, effects of mass loss, binarity, age–metallicity degeneracies, the shape of the IMF, etc. Excellent examples of this type of work and reviews of these difficulties can be found in, among others, Tolstoy & Saha (1996), Aparicio, Gallart & Bertelli (1997), Tolstoy et al. (1998), Gallart et al. (1999a,b), Aparicio, Carrera & Martínez-Delgado (2001), Aparicio & Gallart (2004) and Gallart, Zoccali & Aparicio (2005). These difficulties are especially problematic when the data do not extend to beneath the main-sequence turn-offs (which offer the best handle on the age of the population). Therefore, we keep our analysis intentionally simple and use it only to emphasize that DDO210 cannot contain a majority old population. A more sophisticated analysis is not warranted by the current data given the uncertainties involved.

We use the Bertelli et al. (1994) evolutionary tracks and the bolometric correction libraries of Lejeune, Cuisinier & Buser (1997). We adopt a power-law IMF, $\phi(M) \propto M^{-x}$, with an exponent of $x = -1.35$, -2.2 and -2.7 in the range $M \in$ [0.1, 0.5], [0.5, 1] and [1, 120], respectively. We ignore the effects of binary stars. We construct 10 different SFHs ('partial models'), corresponding to a constant SFR between [0, 0.5], [0.5, 1.5], [1.5, 2.5], [2.5, 3.5], [3.5,

[2] http://iac-star.iac.es/iac-star

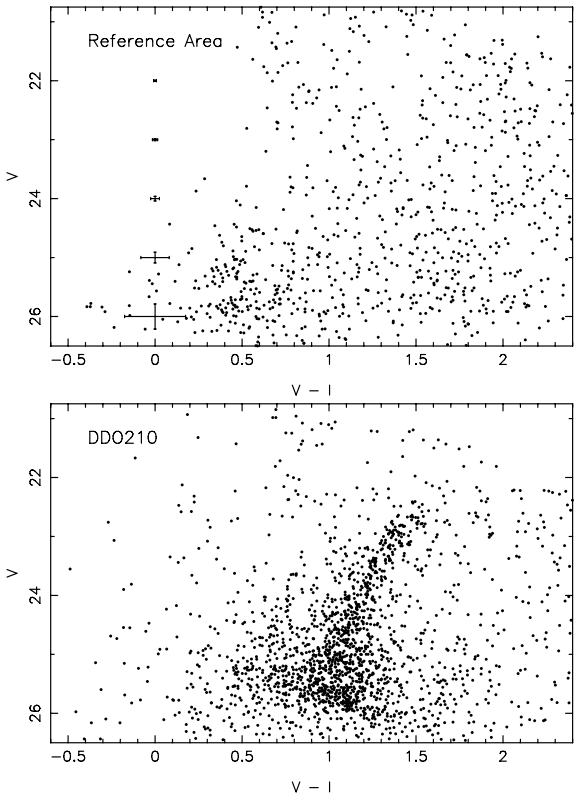

Figure 2. V versus $(V-I)$ CMD for the reference area (top) and for DDO210 (bottom), from our Subaru Suprime-Cam imaging. The reference area is located outside of the innermost 7.5 × 7.5 arcmin^2 of the Suprime-Cam field, and the DDO210 CMD consists of those stars in the innermost 4 × 4 arcmin^2.

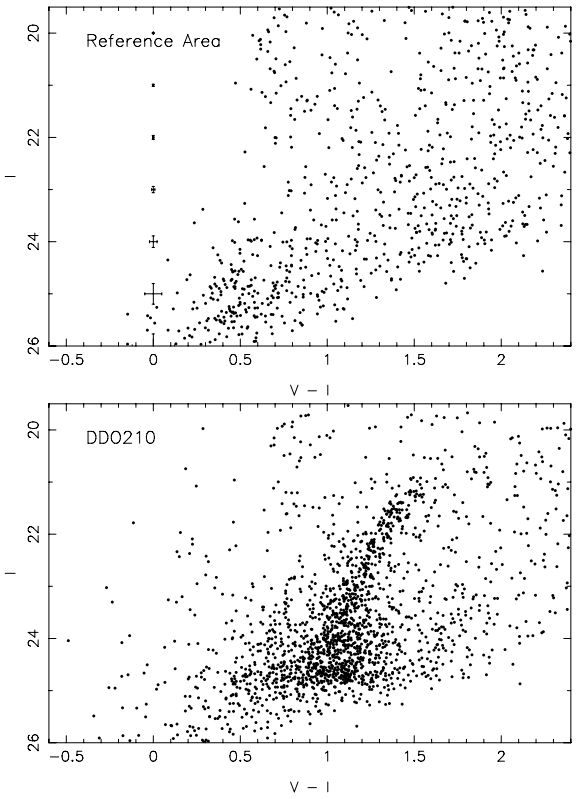

Figure 3. I versus $(V-I)$ CMD for the reference area (top panel) and for DDO210 (bottom panel), from our Subaru Suprime-Cam imaging. The reference area is located outside of the innermost 7.5 × 7.5 arcmin^2 of the Suprime-Cam field, and the DDO210 CMD consists of those stars in the innermost 4 × 4 arcmin^2.

4.5], [4.5, 5.5], [5.5, 6.5], [6.5, 7.5], [7.5, 10] and [10, 13] Gyr ago, with no star formation at all other times. For each interval, the metallicity (chemical enrichment law) is chosen to reproduce the colour of the RGB (Section 3.5). The magnitudes of the model stars are then convolved with the error distribution of our data to facilitate a comparison between the two. The left-hand panel of Fig. 9 shows a CMD of our composite Suprime-Cam/FORS1 data set. The right-hand panel is an illustration of an IAC-STAR model, and shows the Monte Carlo simulation of the 3.5–4.5 Gyr stellar population, normalized to the same number of stars and convolved with our error distribution. We note that a bright ($M_I < -4$ mag), AGB population is produced by this model. This resembles the population of stars just brighter than the TRGB in our data which were discussed at length in Sections 3.1 and 3.2.

The solid histograms in the top panels of Fig. 10 shows the normalized M_I luminosity function for DDO210 in the region of the red clump. The other four panels show the red clump luminosity function for four of our simulated partial SFHs. The youngest (1.5–2.5 Gyr) red clump peaks at a brighter magnitude than the data, although this young population could contribute to the bright side of the DDO210 red clump. Similarly, the 5.5–6.5 Gyr population could contribute to the faint side of the red clump. A single, 1 Gyr, period of star formation at intermediate ages does not produce a red clump with the required magnitude dispersion to match the data. To illustrate this, the dot–dashed histograms overlaid on the top panels of Fig. 10 show the red clump luminosity function for a star formation history (SFH) which is constant between 1.5–3.5 and 4.5–6.5 Gyr,

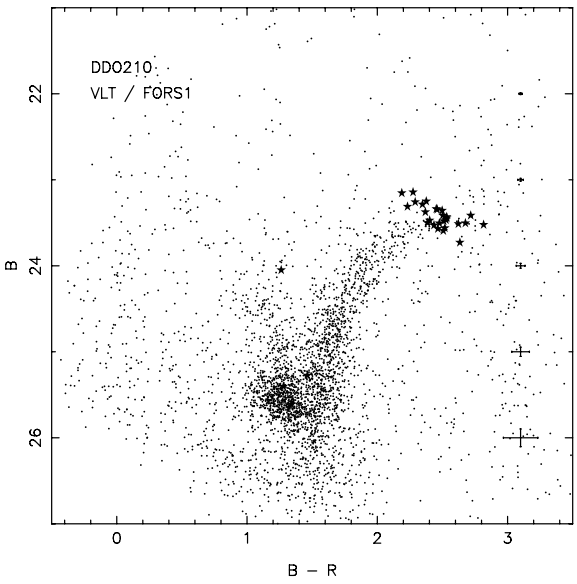

Figure 4. B versus $(B-R)$ CMD for DDO210, from our VLT FORS1 imaging. The highlighted stars have $1.3 < (V-I) < 1.7$ and $20.80 < I < 21.21$, and represent the grouping of stars identified by L99 and K02 as marking the TRGB (Sections 3.1, 3.2). However, the tight grouping of most of these stars in this figure slightly to red of the RGB suggests that it is far more likely that these stars represent an evolved AGB population in DDO210.

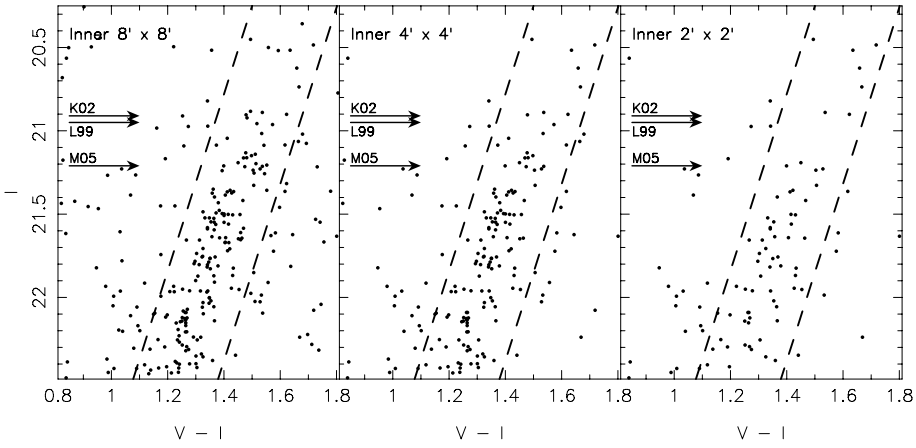

Figure 5. *I*-band CMDs of DDO210 in the region of the TRGB, using different spatial cuts on our Suprime-Cam data. Left-hand panel: only stars located within the central 4×4 arcmin^2 of DDO210; middle panel: only stars located within the central 2×2 arcmin^2 and right-hand panel: only stars located within the central 1×1 arcmin^2. The arrows indicate the location of the TRGB as derived by Karachentsev et al. (2002) (top panel), Lee et al. (1999) (middle panel) and McConnachie et al. (2005) (bottom panel). The feature identified by the former two authors as the TRGB disappears under the more stringent spatial cuts. It is possible that this population represents a weak upper AGB population.

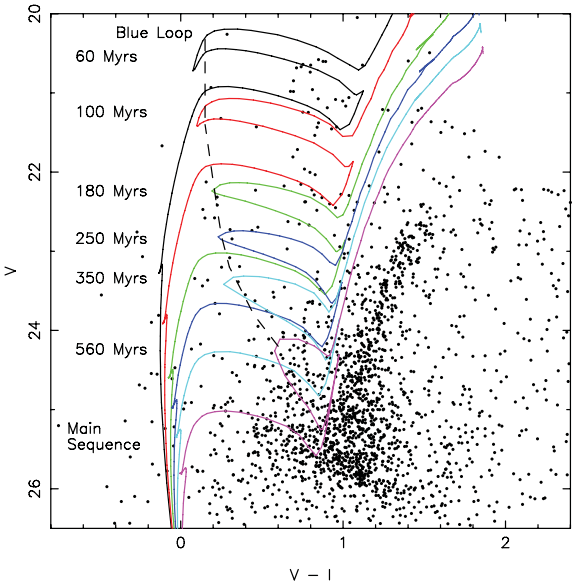

Figure 6. *V* versus $(V - I)$ CMD for DDO210, from our Subaru Suprime-Cam imaging, with Padova isochrones (Girardi et al. 2002) overlaid. These isochrones correspond to [Fe/H] $= -1.3$ and ages of 60, 100, 180, 250, 350 and 560 Myr. The locus of main-sequence stars (with $V < 22.8$ mag, $(V - I) \simeq -0.2$ mag) and the locus of core helium-burning blue-loop stars [with $V < 20$ mag, $(V - I) \simeq 0.2$ mag] are indicated.

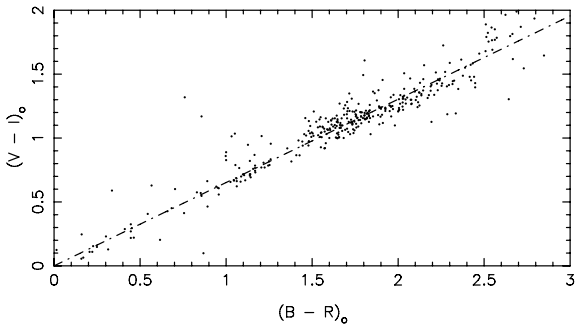

Figure 7. $(V - I)_o$ versus $(B - R)_o$ for all stars reliably identified in all four filters and with uncertainties of $\leqslant 0.05$. The dashed line is the best-fitting linear relationship of $(V - I)_o = 0.652\,(B - R)_o$.

and zero at all other times. This broader, composite SFH reproduces both the *magnitude* and the *shape* of the red clump.

Older stellar populations are shown in the remaining two panels of Fig. 10. The 7.5–10 Gyr red clump consists predominantly of stars fainter than those are seen in the red clump of DDO210. For stars older than 10 Gyr, the region of the CMD, which contains the red clump, contains a lot of HB stars. The luminosity function in this region is significantly fainter than the observed luminosity function. It is clear that, if stars older than ∼7 Gyr are found in DDO210, then their overall contribution to the stellar population of DDO210 must be $\ll$50 per cent. Otherwise, the morphology of the red clump in DDO210 would be notably different. We estimate that, if such a population exists, it probably contributes no more than ∼20–30 per cent. This estimate is unaffected by incompleteness, since the red clump is above our incompleteness limit. However, deeper photometry, which samples some of the older main-sequence turn-offs in DDO210, would be of huge value in providing much stronger limits on the contribution of an ancient stellar population in DDO210.

3.5 The red giant branch and its bump

The most prominent feature in the CMDs displayed in Figs 2–4 is the RGB. This feature is only seen in stellar populations older than a few Gyr, and is an indicator of an intermediate and/or old population. It cannot be used as a more precise indicator than this without certain difficulties, because of the well-known degeneracies of RGB colour with both age and metallicity (redder RGB stars may be older and/or more metal rich than bluer RGB stars). When analysing a CMD, the standard assumption which is used in the absence of other constraints is that the stellar populations which give rise to the RGB are as old as the MW globular clusters. In this case, the colour and colour dispersion of the RGB are due to metallicity variations, and so an estimate of the metallicity may be made. This is usually obtained by a bilinear interpolation of the position of the RGB stars in colour–magnitude space between a set of globular

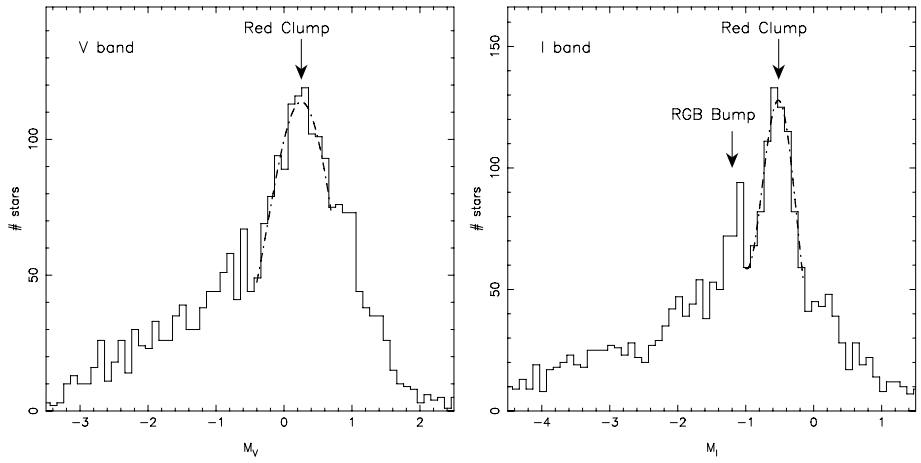

Figure 8. Luminosity functions for M_V and M_I from the composite Suprime-Cam/FORS1 data (see text), with a Gaussian fit to the region of the red clump overlaid as a dot–dashed line on each. The central value of the Gaussian is taken to be the mean magnitude of the red clump. The luminosity functions are not foreground corrected, but the very high stellar densities in the region of interest means that the presence of foreground stars does not affect our measurements of the mean magnitudes of the red clump.

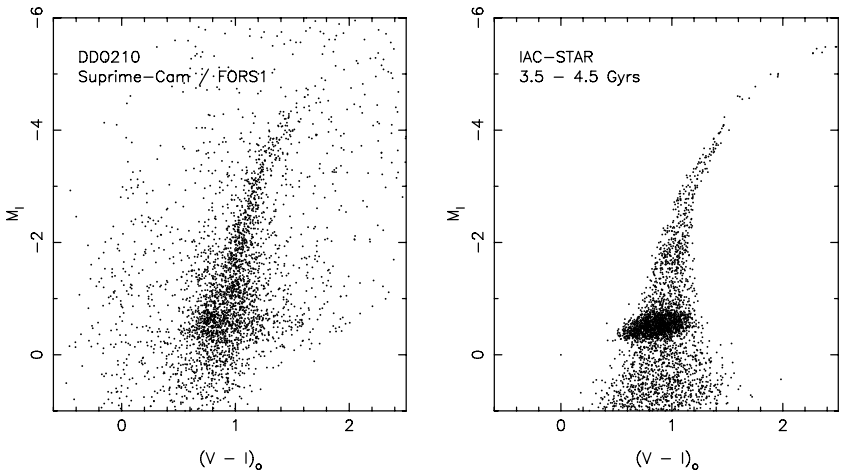

Figure 9. Left-hand panel: M_I versus $(V - I)_o$ CMD using our composite Suprime-Cam/FORS1 data set. The red clump is now clearly visible. Right-hand panel: illustration of a partial SFH model generated with IAC-STAR (Aparicio & Gallart 2004), scaled for the same number of observed stars, and subsequently convolved with our error distribution. This CMD is for the stellar population which formed its stars at a constant rate between 3.5 and 4.5 Gyr ago, and which reproduces the mean magnitude of the red clump very well.

cluster fiducial tracks, isochrones or evolutionary tracks and creating a metallicity distribution function (MDF; e.g. Durrell, Harris & Pritchet 2001). Alternatively, empirical calibrations between RGB colour and metallicity exist which can be easily applied (e.g. Da Costa & Armandroff 1990).

L99 assumed that DDO210 is as old as the MW globular clusters, and derived a mean metallicity of [Fe/H] $= -1.9 \pm 0.1$, where the second term is the error in the mean metallicity, not the metallicity dispersion. Using our Suprime-Cam data, we construct a MDF for DDO210 by interpolating between the Victoria–Regina set of isochrones by VandenBerg, Bergbusch & Dowler (2005) for a 13-Gyr stellar population, with *BVRI* colour–$T_{\rm eff}$ relations as described by VandenBerg & Clem (2003). We use only those stars in the brightest 1.5 mag of the RGB, where the photometric errors are smallest and the colour difference caused by metallicity variations is largest. We find that, under this assumption, the mean metallicity is [Fe/H] $= -1.9$, in agreement with L99. However, from Section 3.4, we know that the majority of stars in DDO210 do not belong to an old population, and that most of the stars have an average age of $\sim$4 Gyr. We therefore repeat our analysis, but this time, compare the RGB stars to isochrones which are 4 Gyr old. The resulting MDF can be seen in the right-hand panel of Fig. 11. The left-hand panel shows a zoomed in view of the RGB of DDO210, with a few of the isochrones which are used overlaid. With this assumption about the age, we find DDO210 has a mean metallicity of [Fe/H] $= -1.3 \pm 0.1$, and a metallicity dispersion of $\sigma_{\rm [Fe/H]} = 0.27$ dex. The latter quantity is likely overestimated, however, since some of the colour variation in the RGB will be due to the age spread which we know exists in DDO210 (Section 3.4.2).

Finally, the RGB bump is clearly visible in the *I*-band luminosity function shown in Fig. 8 at $M_I \simeq -1.2$ mag. It is less obvious in the *V*-band luminosity function, where its magnitude is closer to that of the red clump. However, from the CMD in Fig. 9, its colour is $(V - I) \simeq 1$, and so $M_V \simeq -0.2$ mag. The RGB bump was first discovered in dwarf galaxies by Majewski et al. (1999) in Sculptor (see also Bellazzini, Ferraro & Pancino 2001; Monaco et al. 2002;

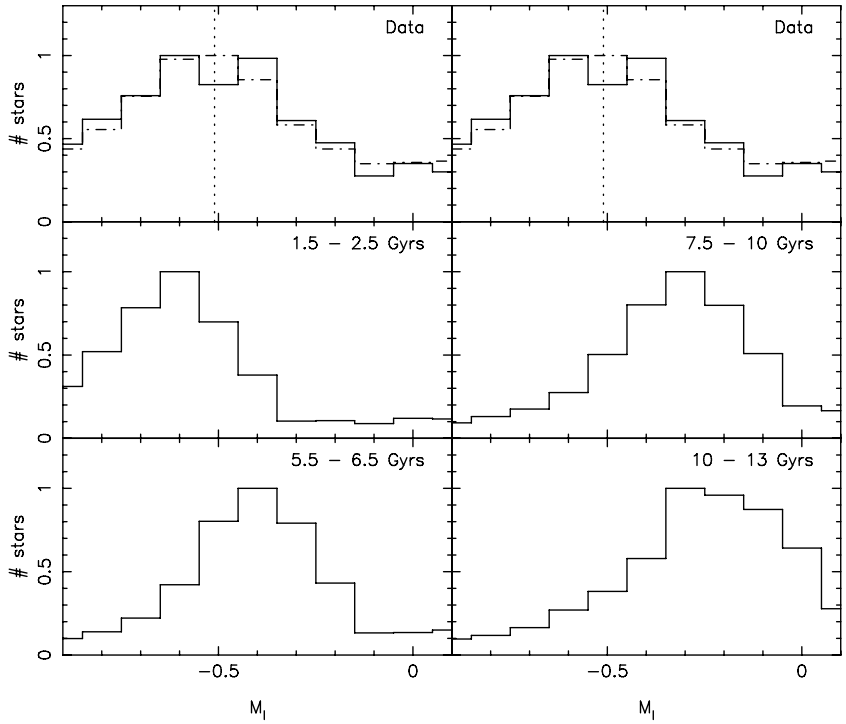

Figure 10. Top panels: M_I luminosity function for the red clump from our composite Suprime-Cam/FORS1 data. The dot–dashed histograms represent a composite stellar population with a constant SFR between 1.5–3.5 and 4.5–6.5 Gyr. Other panels: M_I luminosity functions for red clumps generated with the IAC-STAR tool, convolved with our error distributions. Star formation in these models occurred at a constant rate for the periods indicated, with the metallicity held constant at the value which reproduces the colour of the RGB for those ages. The young – intermediate-age red clumps have peak magnitudes consistent with the broad peak of the observed luminosity function. On the other hand, the older populations produce red clumps which are too faint in comparison to the data. If red clump stars of these ages are present in the data, they must be a minority population. No individual model reproduces the observed red clump luminosity function.

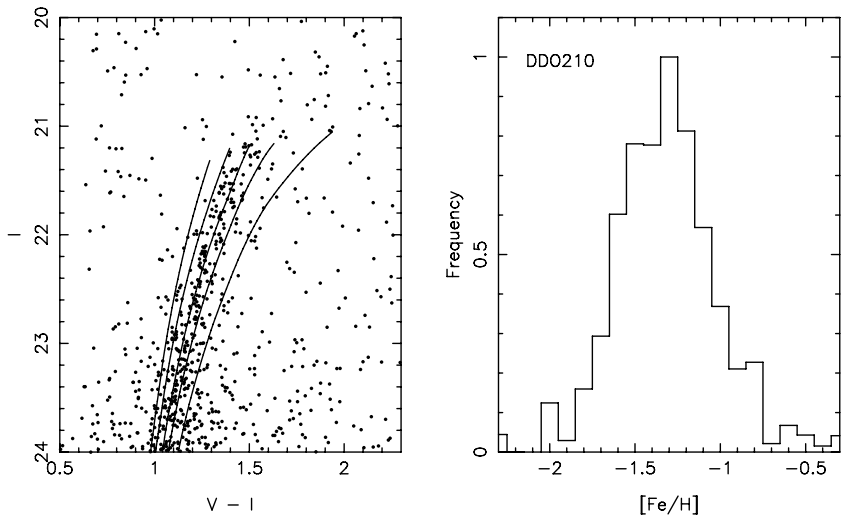

Figure 11. Left-hand panel: the upper RGB of DDO210. Victoria–Regina isochrones by VandenBerg et al. (2005), with *BVRI* colour–$T_{\rm eff}$ relations as described by VandenBerg & Clem (2003), are overlaid. These tracks correspond to an age of 4 Gyr and a metallicity of [Fe/H] $= -2.3, -1.8, -1.4, -1.1$ and -0.8. These are a few of the larger grid of isochrones which we use to construct the MDF. Right-hand panel: MDF for DDO210, derived by interpolation of the colours and magnitudes of the RGB stars in DDO210 with the full grid of Victoria–Regina isochrones corresponding to the 4-Gyr population. The mean metallicity found in this way is [Fe/H] $= -1.3 \pm 0.1$, with a dispersion of $\sigma_{\rm [Fe/H]} = 0.27$ dex.

Bellazzini, Gennari & Ferraro 2005). As the helium-burning core of the RGB star increases in size, so too does the radius of the outer hydrogen-burning shell. The RGB bump represents the point at which this shell encounters the chemical discontinuity left behind by the innermost penetration of the convective envelope. This causes a decrease in luminosity while the hydrogen-burning shell adapts to this new environment, before the star continues its ascent of the RGB. The magnitude of the RGB bump and its dependence on age

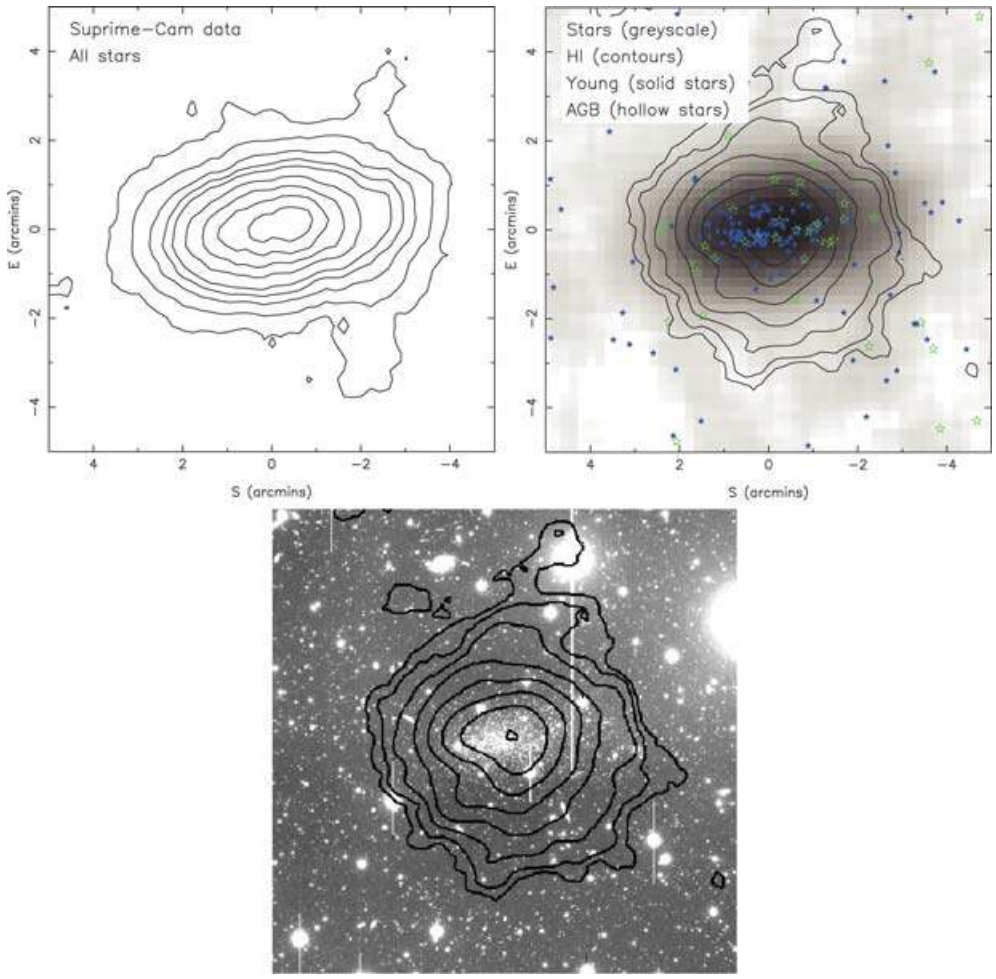

Figure 12. Top left-hand panel: a contour map of the spatial distribution of all stellar sources in DDO210 which have $I_c < 26$ mag. Contour levels are set at 2, 5, 10, 15, 20, 30, 40, 50 and 60σ above the background. Top right-hand panel: H I contours for DDO210, from low-resolution VLA observations by Young et al. (2003). Contour levels are set at 0.1, 0.2, 0.4, 0.8, 1.6, 3.2, 6.4 and 12.8×10^{20} atoms cm^{-2}. The stellar distribution shown in the left-hand panel is included as a linear grey-scale. The solid stars represent the positions of candidate main sequence and blue loop satisfying $I < 24.3$ mag and $(V - I) < 0.5$, and the open stars represent the positions of candidate bright AGB stars, satisfying $1.3 < (V - I) < 1.7$ and $20.80 < I < 21.21$. Bottom panel: the I_c-band Suprime-Cam image of DDO210, with H I contours overlaid. The scale, orientation and contour levels are the same as in the previous panels.

and metallicity have been quantified for MW globular clusters by Ferraro et al. (1999). Using their equation (3), the RGB bump is expected at $M_V = -0.27$ for a population with an age of 4 Gyr and a metallicity of [Fe/H] $= -1.3$. This compares favourably to where we detect the bump in DDO210. To the best of our knowledge, this is the first time that the RGB bump has been observed in a dwarf galaxy beyond the MW satellite system.

4 THE STRUCTURAL CHARACTERISTICS OF DDO210

Our photometric data sets extend over a relatively large area of sky, and the Suprime-Cam data in particular is well suited to studying the global structural properties of DDO210, both in terms of the unresolved light and the resolved stellar components. For example, having shown that DDO210 consists of composite stellar populations, a natural question to ask is *how are these populations spatially distributed?* In this section, we first derive some global parameters for DDO210 based upon both its resolved and unresolved components. We then study the distribution of the various stellar types in DDO210, and finally we compare its stellar structure to its H I distribution, based upon VLA observations by Young et al. (2003).

4.1 The integrated structure

Following the method of McConnachie & Irwin (2006), we have directly estimated the central surface brightness and integrated luminosity of DDO210 from the integrated V' flux distribution. From equation (2), the colour correction to convert to Landolt V is significantly smaller than the final uncertainties in our measurements, and so we can treat our measurements as Landolt V. The object catalogues are used to define a bright foreground star component 1 mag above the TRGB, to allow for the presence of AGB stars. A circular aperture is excised around each foreground star and the flux within this aperture is set to the local sky level, interpolated from a whole-frame background map. The size of this aperture is the maximum of four times the catalogue-recorded area of the bright star at the detection isophote, or a diameter four times the derived full width at half-maximum (FWHM) seeing. Each frame is then re-binned on a

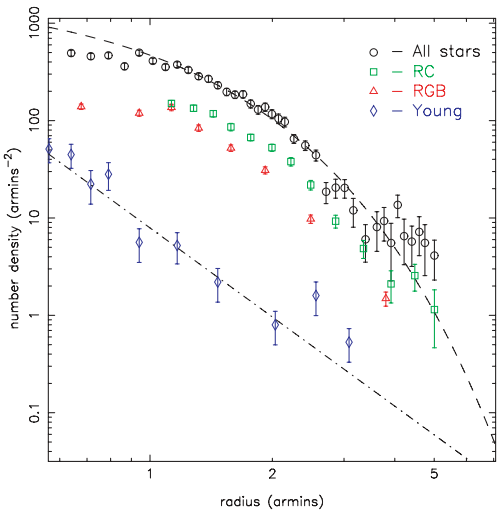

Figure 13. Radial profiles of various stellar populations in DDO210: all stars (black circles), red clump (green squares), RGB stars (red triangles) and young stars (blue diamonds). See text for colour cuts used. The RGB stars and red clump stars follow a similar exponential profile to the overall population (dashed curve). The young stars, however, follow a different radial profile, represented here by a power law (dot–dashed line). Crowding may affect these profiles inside ∼0.8 arcmin.

4×4 grid to effectively create 0.8-arcsec pixels. The binned image is then further smoothed using a 2D Gaussian filter with an FWHM of 5 arcsec.

The result of this procedure is to produce a coarsely sampled smooth image containing both the resolved and unresolved light contribution from DDO210. The central surface brightness can then be measured by deriving the radial profile, here defined as the median flux value within elliptical annuli. Finally, large elliptical apertures are placed over DDO210 and several comparison regions to estimate the background-corrected integrated flux from the dwarf and the reference regions. The variation in the flux from the multiple comparison measures gives a good indication of the flux error, which is, of course, dominated by systematic fluctuations rather than by random noise. This is a particular problem for DDO210 because of the numerous resolved blue stars we observe in this galaxy. To mitigate the effect of random residual foreground stellar haloes and scattered light from bright stars just outside the field of view, the elliptical apertures are chosen to correspond to the derived value of $r_{\frac{1}{2}} = 1.1$ arcmin (Section 4.2). The estimated total flux is then scaled to allow for this correction. The small angular size of DDO210 also allows us to measure the integrated flux by summing over the whole galaxy, which we can then compare with the value derived from within $r_{\frac{1}{2}}$.

Using the flux within $r_{\frac{1}{2}}$, we find that the total magnitude of DDO210 is $V = 14.74 \pm 0.10$ mag, which implies $M_V = -10.58 \pm 0.13$ mag. The total flux obtained on integrating over the entire galaxy is, for comparison, $V = 14.49 \pm 0.10$ mag, implying $M_V = -10.83 \pm 0.13$ mag. We believe that the discrepancy between these two values is a result of the flux in V being centrally concentrated due to a central population of young stars (Section 4.2). The extinction-corrected central surface brightness of DDO210 is $\mu_o = 23.6 \pm 0.2$ mag arcsec^{-2}. These values confirm previous results showing that DDO210 is one of the faintest galaxies in the Local Group.

4.2 The stellar structure

Fig. 1 shows the V- and I-band Suprime-Cam images of DDO210. Although the galaxy is clearly visible at the centre of each field, it is hard to tell from these images how far out its stars extend. In order to probe to fainter surface brightness thresholds, therefore, we construct a contour plot of the resolved stars. This approach can probe several magnitudes fainter in surface brightness than studies based only on the unresolved light (typically $\mu > 31$ mag arcsec^{-2}).

We construct our contour map following the methodology of Irwin & Hatzidimitriou (1995) and McConnachie & Irwin (2006). Briefly, we use all those objects which have been reliably classified as stellar in the I-band of the Suprime-Cam data, and which have $I_c < 26$ mag. We construct an image from this data by binning stars according to their position in a grid with a resolution of 12 arcsec. We then apply a crowding correction to this grid (Irwin & Trimble 1984), such that

$$f' \simeq f\left(1 + 2fA' + \frac{16}{3}f^2A'^2 \ldots\right), \quad (5)$$

where f is the observed number density of *all detected images* (not just stellar), f' is the actual number density and A' is the typical area of the image. Adopting this correction increases the number density of stars in the very central region by a factor of ∼1.7, but has little effect outside the inner ∼1 arcmin.

The top left-hand panel of Fig. 12 shows the contour map of the spatial distribution of the stellar sources in DDO210. A linear filter has been applied to this map to smooth out structures below a scale of 1.4 arcmin. The contour levels have been set at 2, 5, 10, 15, 20, 30, 40, 50 and 60σ above the background. In order to estimate the background level, we constructed a histogram of the intensity distribution of pixels located in the outer parts of the Suprime-Cam field. We then performed a sigma-clipped fit of a Gaussian to this distribution, finding that the background stellar intensity is 32.57 ± 0.14 stars arcmin^{-2}, and $\sigma = 7.71 \pm 0.12$ stars arcmin^{-2}.

DDO210 has a fairly regular overall stellar structure for a dwarf galaxy, with no obvious substructures or irregular-shaped isophotes. Its position angle and ellipticity can be quantified as a function of isophotal threshold in an identical way as in McConnachie & Irwin (2006), making use of standard image-analysis routines to calculate these quantities in a parameter-independent fashion. The position angle of DDO210, measured east from north, is $\theta = 98.^{\circ}7 \pm 1.^{\circ}0$, where the uncertainty indicates the variation in this quantity for the different isophotal thresholds. Clearly, the variation is minimal and no trends, such as isophotal rotation, are observed. The ellipticity ($\epsilon = 1 - b/a$), on the other hand, varies systematically as a function of radius in DDO210, such that the galaxy is more elongated at smaller radius ($\epsilon \sim 0.6$) and more circular at larger radius ($\epsilon \sim 0.4$). Although this effect is not dramatic, it is sufficiently strong that it can be detected by eye in the top left-hand panel of Fig. 12.

The spatial distributions of the various stellar populations identified earlier can also be investigated separately by applying colour cuts on the CMD to isolate the stars belonging to these features. In particular, we isolate the following populations.

(i) RGB stars. These are defined as stellar objects with $21.21 < I < 23.23$ mag, $I > -5.3 \times (V - I) + 28.2$ and $I < -5.3 \times (V - I) + 29.8$.

(ii) Red clump stars. These are defined as stellar objects with $24.3 < I_c < 25.2$ mag.

(iii) Main-sequence and blue-loop stars. These are defined as stellar objects with $I < 24.3$ mag, $(V - I) < 0.5$ mag.

Radial profiles are constructed for each of these populations by counting the number of stars in elliptical annuli, centred on DDO210, with a fixed position angle of $\theta = 98\overset{\circ}{.}7$ and a fixed ellipticity of $\epsilon = 0.5$. Using fixed values for these parameters ensures that the radial profile derived will be robust and suitable for comparison to models. Crowding and background corrections are applied in a similar way as for the contour plot. Results are shown in Fig. 13. Green squares represent the red clump component, red triangles represent the RGB component and blue diamonds represent the young stellar component. Also shown as black circles is the radial distribution of the overall stellar population, defined in the same way as for the contour plot. Error bars show the combined uncertainty of the Poisson error in the counts and the uncertainty in the background estimate. Each bin has a minimum signal-to-noise ratio (S/N) of 10, with the exception of the young stellar profile. Here, the fewer stars available require us to use a lower S/N threshold of 2.5. The radial profiles stop at the point at which they level out, indicating that we can no longer trace the DDO210 population. The inner $\sim 0\overset{\circ}{.}8$ of some of the profiles may be unreliable due to crowding effects, but the outer parts of the profile remain unaffected.

The dashed curve in Fig. 13 is an exponential fit to the overall stellar population of DDO210, and has a scalelength of $r_e = 0.66 \pm 0.02$ arcmin (half-light radius, $r_{\frac{1}{2}} = 1.1 \pm 0.03$ arcmin), corresponding to $r_e = 206 \pm 10$ pc at the distance of DDO210. Only points beyond 1 arcmin were used in the fit to avoid crowding issues. An exponential function with a similar scalelength also matches the RGB and red clump radial profiles equally well ($\chi^2_{\rm reduced} = 1.8$). This is unsurprising, given that most of the stars in DDO210 are red clump or RGB stars, and that it is probable that most of these stars arise in the same star formation episode.

On the other hand, the youngest stars in DDO210 are not distributed in the same way as the older populations. The radial distribution of the main-sequence and blue-loop stars is better approximated by a power law (dot–dashed line), of index $n = -3.0 \pm 0.3$ ($\chi^2_{\rm reduced} = 1.5$). Clearly, the recent star formation in this galaxy occurred in a spatially more concentrated region than the earlier epoch(s) of star formation. This difference in the radial profiles of the young and older stellar populations confirms and quantifies the suggestion by L99 that the central regions of DDO210 have seen an enhancement in the SFR during the last few hundred Myr.

The radial profiles of the older stellar populations in DDO210 bear some similarity to the radial profile of Leo A, derived by Vansevičius et al. (2004). These authors found that, beyond a radius of $\simeq$5.5 arcmin, the slope of the radial profile of Leo A changes and becomes shallower (their fig. 3). They argued that this represented a detection of a halo component in Leo A. DDO210 is sufficiently faint that we are unable to trace the stellar component out to much beyond $\sim$5 arcmin, to see if there is a similar change in slope for this galaxy. The distribution of younger stars in Leo A is also different to its older populations, but in Leo A the gaseous distribution is similar to the RGB stars. As we show in the next section, this is not the case for DDO210.

4.3 The gaseous structure

Given our findings in the previous section, it is interesting to explore the spatial distribution of the gas in DDO210, to see if and how this correlates with the stellar distribution, especially the young stars. The H I content of DDO210 has been relatively well-studied, starting with the survey by Fisher & Tully (1975). More recently, Lo, Sargent & Young (1993) have measured the H I mass in DDO210 to be $3 \times 10^6\,{\rm M}_\odot$. Young et al. (2003) measured the radius to which the H I column density has dropped to 10^{20} atoms cm^{-2}, and compare this to the radius of the 25 mag arcsec^{-2} stellar isophote. They found that the ratio of these H I to optical scalelengths is approximately 2:1, which is typical of dIrr galaxies. The peak column density of H I is likewise typical, at $\sim 1.3 \times 10^{21}$ atoms cm^{-2}. L. Young has kindly sent us her H I data for DDO210, and we have plotted the low-resolution data on to a grey-scale image of the stellar distribution (linear scale) in the top right-hand panel of Fig. 12. Also plotted as individual points in this panel are the candidate main-sequence and blue-plume stars from our Suprime-Cam imaging. The bottom panel of Fig. 12 shows, on the same scale, the H I contours overlaid on the *I*-band Suprime-Cam image of DDO210.

It is clear from Fig. 12 that the overall stellar and H I spatial morphologies of DDO210 are different, insofar as the H I distribution is predominantly spherical, whereas the stellar distribution is much more elliptical. Young et al. (2003) noted that DDO210 displayed a large-scale velocity gradient, and later observations by Begum & Chengalur (2004) measured a rotation curve for the H I, which peaks at $\sim$16 km s^{-1}. The kinematic major axis of the rotation shows significant warping, and its position angle changes substantially with radius. However, this variation generally follows the morphological position angle derived from fits to the H I distribution. At $\sim$2 arcmin from the centre of the H I distribution, the position angles of the kinematic and morphological H I axes are $\sim 95^\circ$, which is in good agreement with the position angle we derive for the stellar distribution. Begum & Chengalur (2004) also derived an inclination for DDO210 of $27^\circ \pm 7^\circ$, based upon the assumption that the actual shape of the H I is circular. Using a similar assumption, we find that the inclination of DDO210 from its stellar distribution varies between $\sim 55^\circ$ and $\sim 65^\circ$, in agreement with L99 and significantly different to the H I value. Based on these numbers, we consider it unlikely that the majority of stars in DDO210 are distributed in a disc, and so the inclination we derive is unlikely to be meaningful. Begum & Chengalur (2004) reached the same conclusion. We note that the fact that most of the stars are radially distributed in an exponential profile is *not* evidence that the stars are distributed in a disc. Although exponential profiles match discs very well, our experience with dSph galaxies shows that these too are well described by exponential profiles (Irwin & Hatzidimitriou 1995; McConnachie & Irwin 2006; see also Faber & Lin 1983). We also note that these findings do not prevent *some* stars in DDO210 from being distributed in a disc.

Young et al. (2003) and Begum & Chengalur (2004) both overlaid their H I contours on optical images of DDO210 and note that the optical component appears to be offset from the H I component. A comparison of the panels of Fig. 12 reveals the cause of this apparent offset. The lower panel shows that the brightest optical emission and the H I contours are not centred on one another, whereas the top two panels show that the overall stellar and H I content of DDO210 are centred on one another. The reason for this disparity is that the *young* stellar component, to which the brightest stars in DDO210 belong, is not clumped in the middle of DDO210, but instead offset a few arcmins to the east. This is easily visible from the top right-hand panel. Since a few young stars contribute far more light than many older stars, the optical emission is biased towards tracing this population, rather than the majority older population. It is interesting to note that the highest density of young stars occurs at a point where there is a slight 'dent' in the H I contours, perhaps suggesting that some event caused the gas to be asymmetrically compressed, triggering off-centre star formation. Alternatively, the off-centre star formation may be due to recently captured gas, which has not become fully virialized. Finally, we also note that the stellar component of

DDO210 is significantly more extended than that suggested by the optical image, and effectively extends out as far as the H I.

5 DISCUSSION: IS THIS THE DAWNING OF THE AGE OF AQUARIUS?

DDO210 is dominated by an intermediate-age stellar population. In this respect, it resembles Leo A, another relatively isolated Local Group galaxy which has been shown to consist of a predominantly young (<2 Gyr) stellar population (Tolstoy et al. 1998). Leo A is located ∼690 kpc from the MW (Mateo 1998), and it is conceivable that it is on a highly radial orbit around the MW. Interactions may have affected its SFH. In particular, the presence of RR Lyrae stars in Leo A shows that it has an old component, and may well have had ongoing, low-level, star formation until a few Gyr ago, when the star formation rate increased. This may have been brought on by a close encounter with the MW which triggered enhanced star formation.

DDO210, on the other hand, is even more isolated than Leo A, and external tidal effects from the MW and M31 cannot have played a significant role in its evolution (equation 1). Interactions are not likely to have affected its observable properties, and so its unusual SFH must be explained without recourse to interactions. The total mass of DDO210 is important to consider as well, since its circular velocity is $\sim$16 km s^{-1}, implying a mass of $\sim 10^{7-8}$ M$_\odot$ (Begum & Chengalur 2004). DDO210 is an intrinsically low-mass galaxy which has not interacted with large masses, and yet it did not form most of its stars until ∼4 Gyr ago.

What seems clear is that DDO210 must have accreted its gas prior to reionization, since it is far too low mass to successfully accrete gas post-reionization. Since the virial temperature of DDO210's halo will not have been vastly higher than the temperature of the accreted gas, the gas will probably have remained in a relatively diffuse configuration in the dark matter halo. What star formation occurred at these early times (if any) will have been small and will have been confined to localized gaseous overdensities, rather than acting on a global scale. Deeper observations are required to determine the exact fraction of old stars in this galaxy. Since the gas never really collapsed all the way to the centre of this system, then a bona-fide disc will not have had a chance to form. This would explain why we, along with others, conclude that it is unlikely that the dominant structure in DDO210 is a disc.

Why most stars are of intermediate age? It could be that DDO210 continued to accrete mass (but not gas) post-reionization, such that eventually the gas collapsed sufficiently that star formation proceeded at a reasonable rate and formed the dominant intermediate-age component. Alternatively, it may be that the gas eventually collapsed sufficiently without the overall mass of DDO210 increasing, either through random perturbations or via normal cooling mechanisms.

The above is, of course, speculation, but a scenario such as this seems plausible given our results and the current cosmological paradigm. As well as the dominant intermediate-age population, however, the recent SFH of DDO210 is also unusual. The current SFR in DDO210 is basically zero (<0.000003 M$_\odot$ yr^{-1}; van Zee et al. 1997; Young et al. 2003), even though this galaxy was forming stars as recently as a few tens of Myr ago. We quantify this apparent inconsistency by assuming DDO210 has formed all of its young stars within the past 500 Myr. We compare the number of young stars observed in the colour–magnitude range $(V - I) < 0.5$, $I < 24.3$ mag with the corresponding number in an IAC-STAR simulation, convolved with our error distribution, which has a constant SFR over the last 500 Myr. In order to match the number of young stars observed, the average SFR over the last 500 Myr must be $\sim$0.0002 M$_\odot$ yr^{-1} i.e. nearly two orders of magnitude larger than the derived upper limit on the current SFR. It could be that the recent SFH of DDO210 is best characterized by a very low, relatively constant SFR, interrupted by periods of inactivity. This 'gasping' star formation scenario has already been implied for several other Local Group galaxies (e.g. Tosi et al. 1991).

The young stars in DDO210 are not centred in the middle of the galaxy, but are offset a few arcmin to the east. This location is coincident with a slight dent in the H I, and perhaps suggests that some recent event, such as an interaction, could have triggered off-centre star formation in this galaxy (although what could have interacted with DDO210 is a mystery!). Alternatively, the off-centre star formation may be due to recently captured gas, which has not yet become fully virialized. The fact that the young stars are still clumped on a scale of ∼1 arcmin (∼0.3 kpc) suggests that they were probably born with a relatively small velocity dispersion ($\sigma \sim$ 3–6 km s^{-1}). We note that Dohm-Palmer et al. (2002) showed that the recent star formation in Sextans A was not confined to the centre of the galaxy, and seemed to migrate with time. They argued that star formation in one part of a cloud could cause star formation in another part of the cloud, by triggering instabilities in the gas. In this case, no interactions would be required to explain the spatial location of the young stars, which would reconcile our finding with the splendid isolation of DDO210.

Finally, we note that the presence of a spatially extended intermediate-age population and a centrally concentrated young population is compelling evidence for the presence of multiple structural components in DDO210. The systematic change in the ellipticity of DDO210 as a function of radius supports this claim. These findings provide yet more evidence that dwarf galaxies are not simple single component stellar systems (e.g. Sculptor, Tolstoy et al. 2004; Leo A, Vansevičius et al. 2004; NGC 6822, Demers, Battinelli & Kunkel 2005; Andromeda II, McConnachie & Irwin 2006).

6 SUMMARY

We have used deep *VI* imaging from the Subaru Suprime-Cam wide-field camera, and *BR* imaging from VLT FORS1, to analyse the stellar content, SFH and structural properties of the low-mass, isolated, Local Group transition-type dwarf galaxy DDO210. We confirm the distance modulus of this galaxy to be $(m - M)_o = 25.15 \pm 0.08$ mag. Main-sequence and blue-loop stars are consistent with having formed within the past 60 Myr, whereas the luminosity of the brightest AGB stars show that this galaxy must have been forming stars within the past 3–6 Gyr. This is consistent with the age estimate derived from the mean *I*-band magnitude of the red clump, which shows that the majority of stars have an average age of 4^{+2}_{-1} Gyr. From the shape of the red clump, we estimate that any contribution from stars with ages $\geqslant$7 Gyr, if present at all, cannot amount to more than ∼20–30 per cent. We discuss the implications of this rather unusual SFH within the cosmological context of dwarf galaxies. In this respect, DDO210 provides a useful insight into star formation in low-mass haloes, since tidal effects cannot have affected the evolution of this isolated system.

The young stars in DDO210 have a different radial distribution to the intermediate-age population, and are offset to the east of this older population. When compared with the spatial distribution of H I, we find that the highest density of young stars is coincident with an apparent 'dent' in the H I contours. In addition, the strong difference in the radial distribution of the intermediate-age stars compared with

the centrally concentrated young population, supports the idea that DDO210 consists of multiple structural components. Clearly, dwarf galaxies are not simple stellar systems.

ACKNOWLEDGMENTS

We thank the referee, Myung Gyoon Lee, for a careful reading and helpful comments. This work has made use of the IAC-STAR Synthetic CMD computation code. IAC-STAR is supported and maintained by the computer division of the Instituto de Astrofsica de Canarias. We are grateful to Lisa Young for sending us her H I data which we have used in this paper, and to Myung Gyoon Lee for providing their photometry of DDO210 to allow for the comparison between data sets. AM would like to thank Kim Venn and Jorge Penarrubia for enjoyable discussions during the preparation of this work, James Bullock for insight into linking cosmology with star formation histories and Sara Ellison and Julio Navarro for financial support. This work is partly supported by a Grant-in-Aid for Science Research (No.16540223) by the Japanese Ministry of Education, Culture, Sports, Science and Technology.

REFERENCES

Aparicio A., Gallart C., 2004, AJ, 128, 1465
Aparicio A., Gallart C., Bertelli G., 1997, AJ, 114, 680
Aparicio A., Carrera R., Martínez-Delgado D., 2001, AJ, 122, 2524
Barker M. K., Sarajedini A., Harris J., 2004, ApJ, 606, 869
Begum A., Chengalur J. N., 2004, A&A, 413, 525
Bellazzini M., Ferraro F. R., Pancino E., 2001, ApJ, 556, 635
Bellazzini M., Gennari N., Ferraro F. R., 2005, MNRAS, 360, 185
Belokurov V. et al., 2006, ApJ, 647, L111
Bertelli G., Bressan A., Chiosi C., Fagotto F., Nasi E., 1994, A&AS, 106, 275
Bullock J. S., Kravtsov A. V., Weinberg D. H., 2000, ApJ, 539, 517
Cole A. A., 1998, ApJ, 500, L137
Da Costa G. S., Armandroff T. E., 1990, AJ, 100, 162
de Vaucouleurs G., de Vaucouleurs A., Buta R., 1983, AJ, 88, 764
Demers S., Battinelli P., Kunkel W. E., 2006, ApJ, 636, L85
Dohm-Palmer R. C., Skillman E. D., Mateo M., Saha A., Dolphin A., Tolstoy E., Gallagher J. S., Cole A. A., 2002, AJ, 123, 813
Durrell P. R., Harris W. E., Pritchet C. J., 2001, AJ, 121, 2557
Einasto J., Saar E., Kaasik A., Chernin A. D., 1974, Nat, 252, 111
Faber S. M., Lin D. N. C., 1983, ApJ, 266, L17
Ferraro F. R., Messineo M., Fusi Pecci F., de Palo M. A., Straniero O., Chieffi A., Limongi M., 1999, AJ, 118, 1738
Fisher J. R., Tully R. B., 1975, A&A, 44, 151
Gallart C., Freedman W. L., Aparicio A., Bertelli G., Chiosi C., 1999a, AJ, 118, 2245
Gallart C. et al., 1999b, ApJ, 514, 665
Gallart C., Zoccali M., Aparicio A., 2005, ARA&A, 43, 387
Girardi L., Bertelli G., Bressan A., Chiosi C., Groenewegen M. A. T., Marigo P., Salasnich B., Weiss A., 2002, A&A, 391, 195
Girardi L., Salaris M., 2001, MNRAS, 323, 109
Girardi L., Groenewegen M. A. T., Weiss A., Salaris M., 1998, MNRAS, 301, 149
Gnedin N. Y., Kravtsov A. V., 2006, ApJ, 645, 1054
Grebel E. K., Gallagher J. S., Harbeck D., 2003, AJ, 125, 1926
Greggio L., Marconi G., Tosi M., Focardi P., 1993, AJ, 105, 894
Hopp U., Schulte-Ladbeck R. E., 1995, A&AS, 111, 527
Hurley-Keller D., Mateo M., Nemec J., 1998, AJ, 115, 1840
Irwin M., Hatzidimitriou D., 1995, MNRAS, 277, 1354
Irwin M. J., Trimble V., 1984, AJ, 89, 83
Karachentsev I. D. et al., 2002, A&A, 389, 812 (K02)
Kauffmann G., White S. D. M., Guiderdoni B., 1993, MNRAS, 264, 201
Klypin A., Kravtsov A. V., Valenzuela O., Prada F., 1999, ApJ, 522, 82
Kravtsov A. V., Gnedin O. Y., Klypin A. A., 2004, ApJ, 609, 482
Lee M. G., Freedman W. L., Madore B. F., 1993, ApJ, 417, 553
Lee M. G., Aparicio A., Tikonov N., Byun Y., Kim E., 1999, AJ, 118, 853 (L99)
Lejeune T., Cuisinier F., Buser R., 1997, A&AS, 125, 229
Lo K. Y., Sargent W. L. W., Young K., 1993, AJ, 106, 507
Majewski S. R., Siegel M. H., Patterson R. J., Rood R. T., 1999, ApJ, 520, L33
Marconi G., Focardi P., Greggio L., Tosi M., 1990, ApJ, 360, L39
Mateo M. L., 1998, ARA&A, 36, 435
Mayer L., Governato F., Colpi M., Moore B., Quinn T., Wadsley J., Stadel J., Lake G., 2001a, ApJ, 559, 754
Mayer L., Governato F., Colpi M., Moore B., Quinn T., Wadsley J., Stadel J., Lake G., 2001b, ApJ, 547, L123
McConnachie A. W., Irwin M. J., 2006, MNRAS, 365, 1263
McConnachie A. W., Irwin M. J., Ferguson A. M. N., Ibata R. A., Lewis G. F., Tanvir N., 2004, MNRAS, 350, 243
McConnachie A. W., Irwin M. J., Ferguson A. M. N., Ibata R. A., Lewis G. F., Tanvir N., 2005, MNRAS, 356, 979 (M05)
McConnachie A. W., Arimoto N., Irwin M. J., 2006, MNRAS, submitted
Méndez B., Davis M., Moustakas J., Newman J., Madore B. F., Freedman W. L., 2002, AJ, 124, 213
Monaco L., Ferraro F. R., Bellazzini M., Pancino E., 2002, ApJ, 578, L47
Moore B., Quinn T., Governato F., Stadel J., Lake G., 1999, MNRAS, 310, 1147
Mould J., Aaronson M., 1979, ApJ, 232, 421
Mould J., Aaronson M., 1980, ApJ, 240, 464
Paczynski B., Stanek K. Z., 1998, ApJ, 494, L219
Rejkuba M., Da Costa G. S., Jerjen H., Zoccali M., Binggeli B., 2006, A&A, 448, 983
Ricotti M., Gnedin N. Y., 2005, ApJ, 629, 259
Sakai S., Madore B. F., Freedman W. L., 1996, ApJ, 461, 713
Schlegel D. J., Finkbeiner D. P., Davis M., 1998, ApJ, 500, 525
Stephens A. W., Frogel J. A., 2002, AJ, 124, 2023
Susa H., Umemura M., 2004, ApJ, 600, 1
Tolstoy E., Saha A., 1996, ApJ, 462, 672
Tolstoy E. et al., 1998, AJ, 116, 1244
Tolstoy E., Gallagher J., Greggio L., Tosi M., de Marchi G., Romaniello M., Minniti D., Zijlstra A., 2000, The Messenger, 99, 16
Tolstoy E. et al., 2004, ApJ, 617, L119
Tosi M., Greggio L., Marconi G., Focardi P., 1991, AJ, 102, 951
Udalski A., Szymanski M., Kubiak M., Pietrzynski G., Wozniak P., Zebrun K., 1998, Acta Astron., 48, 1
van den Bergh S., 1959, Publ. David Dunlop Obs., 2, 147
van den Bergh S., 1979, Memorie della Societa Astronomica Italiana, 50, 11
van den Bergh S., 1999, A&AR, 9, 273
van Zee L., Haynes M. P., Salzer J. J., 1997, AJ, 114, 2479
VandenBerg D. A., Clem J. L., 2003, AJ, 126, 778
VandenBerg D. A., Bergbusch P. A., Dowler P. D., 2006, ApJS, 162, 375
Vansevičius V. et al., 2004, ApJ, 611, L93
Willman B. et al., 2005, ApJ, 626, L85
Willman B. et al., 2006, preprint (astro-ph/0603486)
Yahil A., Tammann G. A., Sandage A., 1977, ApJ, 217, 903
Young L. M., van Zee L., Lo K. Y., Dohm-Palmer R. C., Beierle M. E., 2003, ApJ, 592, 111
Zucker D. B. et al., 2004, ApJ, 612, L121
Zucker D. B. et al., 2006a, ApJ, 643, L103
Zucker D. B. et al., 2006b, preprint (astro-ph/0601599)

This paper has been typeset from a TEX/LATEX file prepared by the author.